Brief Communications

Altered Distribution of Juxtaparanodal $K_v1.2$ Subunits Mediates Peripheral Nerve Hyperexcitability in Type 2 Diabetes Mellitus

Jennifer Zenker,[1,2] Olivier Poirot,[1] Anne-Sophie de Preux Charles,[1] Estelle Arnaud,[1] Jean-Jacques Médard,[1] Catherine Lacroix,[3] Thierry Kuntzer,[4] and Roman Chrast[1]

[1]Department of Medical Genetics and [2]Graduate Program in Neurosciences, University of Lausanne, CH-1005 Lausanne, Switzerland, [3]Centre de Référence des Neuropathies Amyloides et autres Neuropathies Rares, Laboratoire de Neuropathologie, Centre Hospitalier Universitaire de Bicêtre, 94275 Le Kremlin Bicêtre, France, [4]Department of Clinical Neurosciences, Centre Hospitalier Universitaire Vaudois and University of Lausanne, CH-1005 Lausanne, Switzerland

Peripheral nerve hyperexcitability (PNH) is one of the distal peripheral neuropathy phenotypes often present in patients affected by type 2 diabetes mellitus (T2DM). Through *in vivo* and *ex vivo* electrophysiological recordings in db/db mice, a model of T2DM, we observed that, in addition to reduced nerve conduction velocity, db/db mice also develop PNH. By using pharmacological inhibitors, we demonstrated that the PNH is mediated by the decreased activity of K_v1-channels. In agreement with these data, we observed that the diabetic condition led to a reduced presence of the $K_v1.2$-subunits in juxtaparanodal regions of peripheral nerves in db/db mice and in nerve biopsies from T2DM patients. Together, these observations indicate that the T2DM condition leads to potassium channel-mediated PNH, thus identifying them as a potential drug target to treat some of the DPN related symptoms.

Introduction

Diabetic peripheral neuropathy (DPN) is characterized by either "positive" (paresthesia, dysesthesia, allodynia, cramps, fasciculations) and/or "negative" (hypesthesia, anesthesia, tiredness, muscle weakness) symptoms (Quasthoff, 1998). Previous studies suggested that changes in neuronal ion channel expression and function may contribute to DPN symptoms (Quasthoff, 1998; Misawa et al., 2005, 2009). In myelinated axons, ion channels are localized at specific spatially restricted domains (Salzer, 2003). Sodium channels (Na_v), predominantly containing the α-subunit $Na_v1.6$, are clustered at the node of Ranvier and play a critical role in the conduction of the action potential. The juxtaparanodal region is enriched in voltage-gated Shaker-like potassium channels (K_v1) that are responsible for the fast potassium conductance in axons. In addition, nodal K_v7 channels were recently shown to mediate the slow axonal potassium conductance (Schwarz et al., 2006). While previous clinical electrophysiological studies suggested that peripheral nerve hyperexcitability (PNH), which is part of the distal peripheral neuropathy phenotype present in type 2 diabetes mellitus (T2DM), is a consequence of alterations in voltage-gated channels (Misawa et al., 2005, 2009), more direct evidence is lacking.

Approximately 90% of all diabetic patients suffer from T2DM (Nolan et al., 2011). We therefore decided to get more insight into the DPN associated with this form of diabetes by studying a rodent model of T2DM, the db/db mice (Hummel et al., 1966). Our characterization of db/db animals by electrophysiological recordings revealed the presence of PNH as part of their DPN phenotype. We observed that the altered K_v1-channel function contributes to the PNH phenotype in db/db animals and that these functional changes are paralleled by altered distribution of the juxtaparanodal $K_v1.2$-subunit in peripheral nerves of db/db mice and in nerve biopsies from T2DM patients indicating the clinical relevance of our observations.

Materials and Methods

Animals. Db/db breeding pairs were obtained from Janvier, France [B6.BKS(D)-Leprdb/J; Stock Number: 000697] and the generated animals were genotyped as previously described (http://jaxmice.jax.org/strain/000642.html). All animals were housed in a controlled environment with a 12 h light/12 h dark cycle and free access to water and standard laboratory diet. Experiments were performed in accordance with the legal requirements of the University of Lausanne and the Canton of Vaud.

Only male mice were used in this study. Tail vein blood glucose was determined with a glucometer Ascencia Contour (Bayer). Plasma insulin levels were measured by using the Rat/Mouse Insulin ELISA Kit

Received Feb. 14, 2012; revised March 23, 2012; accepted April 9, 2012.

Author contributions: J.Z., O.P., and R.C. designed research; J.Z., O.P., A.-S.d.P.C., E.A., and J.-J.M. performed research; C.L. and T.K. contributed unpublished reagents/analytic tools; J.Z., O.P., C.L., and R.C. analyzed data; J.Z., O.P., A.-S.d.P.C., T.K., and R.C. wrote the paper.

This work was supported by a grant from the Swiss National Science Foundation to R.C. (Grant 31003A_135735/1). We thank the Cellular Imaging Facility of the University of Lausanne for help with the confocal microscopy and Dr. Jérome Devaux for helpful discussions.

Correspondence should be addressed to Roman Chrast, Department of Medical Genetics, Faculty of Biology and Medicine, University of Lausanne, Rue du Bugnon 27, CH-1005 Lausanne, Switzerland. E-mail: roman.chrast@unil.ch.

A.-S. de Preux Charles' present address: Department of Physiology, University of California, San Francisco, San Francisco, CA 94158.

DOI:10.1523/JNEUROSCI.0719-12.2012

 0270-6474/12/327493-06$15.00/0

from Millipore (catalog #EZRMI-13K) according to the manufacturer's protocol.

Human biopsies. All donors gave a written consent for the biopsy. Biopsies of the peroneal nerve and adjacent muscle were performed under local anesthesia, fixed in 3.6% glutaraldehyde and embedded in paraffin for routine analysis, or were embedded in plastic for semithin and ultrathin sectioning, analyzed by light and electron microscopy respectively. Paraffin sections were stained with hematoxylin-eosin and Masson's trichrome. Semithin sections were stained with thionine blue.

Electrophysiology. Nerve conduction velocity recordings and *ex vivo* compound action potential (CAP) recordings have been performed as previously described (Cartoni et al., 2010; de Preux Charles et al., 2010). For pharmacological analysis, the isolated nerves were exposed to the drugs between 30 min and 1 h until the effects seemed stable. Tetrodotoxin (TTX) was purchased from Enzo Life Sciences, tetraethylammonium (TEA) and 4-aminopyridine (4-AP) from Sigma, and flupirtine from Tocris Bioscience. All other chemicals were purchased from VWR.

Immunohistochemistry. Mouse tissues were processed as described previously (Arnaud et al., 2009). Twenty-micrometer-thick sciatic nerve sections were prepared and fixed with Zamboni's fixative for 15 min at room temperature (RT). For immunostainings, the following primary antibodies were used: K_v1.2 (1:200; NeuroMab, K14/16), pan-Na_v (1:100; Sigma, SP19 S6936), $K_v\beta$2 (1:100, Alomone, APC-117), K_v1.1 (1:100; Alomone, APC-009) and MBP (1:100, Millipore Bioscience Research Reagents, MAB386) with the appropriate fluorescent secondary antibodies (Alexa Fluor 594 or 488 conjugated anti-rabbit, anti-mouse or anti-rat at a dilution of 1:200; Invitrogen). Nile Red staining on teased fibers was performed as previously described (Arnaud et al., 2009).

Quantitative PCR. RNA extraction, reverse transcription and qPCR conditions have been performed as previously described (Arnaud et al., 2009). The primers used were as follows: forward 5′-CTGGTACCCATCTGCAAG-3′, reverse 5′-GTGTGCTCTAGGACTGGATG-3′ for K_v1.2; forward 5′-AAGGACGGGAAACGCGAGGG-3′, reverse 5′-ATCGATGGACGCTGGCGGG-3′ for K_v1.1; forward 5′-AGACAGGCTCCCCCGGGATG-3′, reverse 5′-CATGGCCCGCACGGTCTCTTC-3′ for $K_v\beta$2; forward 5′-ACACTAGTGGAAGAGCTGGA-3′, reverse 5′-ACGATCAGGTTCACAATCTC-3′ for Na_v1.6; forward 5′-TTCACAAGTCTTCTAAGGACTCCTCG-3′, reverse 5′-GCACTGGCGTCTGCCG-3′ for MPZ and forward 5′-TTGCTCTTCGTCTCCACCATC-3′, reverse 5′-TCGTGTGTCCATTGCCCAC-3′ for PMP22. Results were normalized by using the reference gene β-actin (forward primer: 5′-GCCCTGAGGCTCTTTTCCAG-3′; reverse primer: 5′-TGCCACAGGATTCCATACCC-3′).

Western blot analysis. Sciatic nerve endoneurium and dorsal root ganglia (DRG) isolated from mice at 23 weeks of age from at least three animals per genotype were pooled and lysed in ice-cold lysis buffer (20 mM $Na_2H_2PO_4$, 250 mM NaCl, 1% Triton X-100, SDS 0.1%) supplemented with Complete protease inhibitors (Roche). After spin down for 15 min at 4°C, proteins were extracted from the supernatant. Protein levels were quantified using the Bio-Rad protein assay with BSA as a standard. Equal amounts of protein extracts were boiled for 5 min at 95°C and were then resolved by 12% SDS-PAGE and electro-transferred onto a polyvinylidene difluoride membrane (GE Healthcare). Membrane was blocked in Tris-buffered saline containing 0.1% Tween (TBS-T) supplemented with 5% milk powder for 1 h at RT, and subsequently incubated overnight at 4°C in the same buffer supplemented with antibodies against K_v1.2 (1:500; NeuroMab, K14/16), and standardized using β-Actin (1:2000; Sigma, A5316) or α/β-Tubulin (1:1000, Cell Signaling Technology, #2148). After washing in TBS-T, blots were exposed to the appropriate horseradish peroxidase-conjugated secondary antibodies (Dako) in the blocking buffer for 1 h at RT. Finally, the blots were developed using ECL reagents (Pierce) and Kodak Scientific Imaging Films (Kodak).

Morphometric analysis. Morphometric analysis, including the g-ratio calculation, was performed as previously described (Arnaud et al., 2009).

Statistics. All data are presented as mean ± SEM. *P* values have been calculated with the Student's *t* test.

Results

Our characterization of db/db mice revealed an increase in body weight and blood glucose levels at 6 weeks of age. To study the consequences of T2DM on peripheral nerve function, we exposed the db/db mice to hyperglycemia for 16 weeks (this, based on the estimated lifespan, represents ~10 years in humans). Therefore, we performed all physiological analysis using 23-week-old mice. At this age, db/db mice were severely obese and hyperglycemic. The initial insulin resistance was followed by a β-cell dysfunction leading to a decline in the plasma insulin levels in db/db mice. Nerve conduction measurements on the sciatic nerve, containing both motor and sensory fibers, revealed a significantly reduced motor nerve conduction velocity (from 40.15 ± 3.49 m/s^{-1} in wild-type (WT) to 30.02 ± 4.46 m/s^{-1} in db/db mice, $p < 0.05$) and we also detected a reduction in the tail sensory nerve conduction velocity (27.32 ± 2.48 m/s^{-1} in WT; 18.62 ± 2.44 m/s^{-1} in db/db mice, $p < 0.05$). Interestingly, the stimulus threshold to initiate a first response during the motor nerve conduction studies was significantly lower in db/db mice compared with WT mice ($p < 0.0003$), indicating hyperexcitability of db/db nerves (Fig. 1*a*). However, the area and amplitude of the compound muscle action potential were not altered in db/db mice compared with WT mice at 23 weeks of age (data not shown).

We extended our above mentioned *in vivo* electrophysiological characterization by *ex vivo* CAP recordings (Stys et al., 1991) on sciatic nerves of 23-week-old mice. The normalized A$\alpha\beta$ CAP amplitude/stimulus strength curves confirmed the presence of an increased excitability in db/db nerves (Fig. 1*b*,*c*). The threshold (Fig. 1*c*, see inset) and the stimulus to get 50% of the maximal CAP amplitude (stim1/2) were significantly reduced ($p < 0.001$). We observed similar results with thinly myelinated Aδ sensory fibers (Fig. 1*d*).

A decrease of fast K_v1-currents in several disease situations was previously described to induce PNH (Arimura et al., 2002; Tomlinson et al., 2010; Shibuya et al., 2011). Therefore, we evaluated the contribution of K_v1-channels to PNH in T2DM by exposing isolated sciatic nerves to 4-AP (500 μM) and DTX-1 (100 nM), which were previously used to block these channels in axons (Röper and Schwarz, 1989; Vabnick et al., 1999). As expected, in WT nerves, K_v1-channel block with 4-AP (Fig. 1*b*,*e*) induced hyperexcitability. The threshold (Fig. 1*e*, see inset) and stim1/2 were significantly reduced ($p < 0.001$). Interestingly, db/db nerve excitability was only barely affected by 4-AP (Fig. 1*b*,*e*). Moreover, we observed a similar lack of 4-AP effect on db/db refractory period (RP; Fig. 1*f*). DTX-1 changed nerve excitability and RP of WT and db/db nerves in a similar way but was less potent than 4-AP (Fig. 1*g*,*h*), probably as a consequence of its previously described more limited diffusion to juxtaparanodal channels (Devaux and Gow, 2008). Together these results suggest a decreased function of K_v1-channels in db/db mice that could be responsible for the observed PNH.

We evaluated the possibility that other ion channels might be implicated in PNH. Previous studies suggested that PNH in diabetic patients could be a consequence of increased persistent nodal Na_v-currents (Misawa et al., 2009). As these currents are mainly mediated by Na_V1.9 TTX-resistant (TTX-R) Na_v-channels (Matsutomi et al., 2006), we tested the sensitivity of CAPs to TTX. The residual CAP amplitude was similar in WT and db/db nerves after exposure to 100 nM TTX (respectively 38 ± 2% and 37 ± 6%) and 1 μM TTX (<2% for both tested genotypes). As mutations affecting nodal K_v7.2 lead to PNH (Taylor

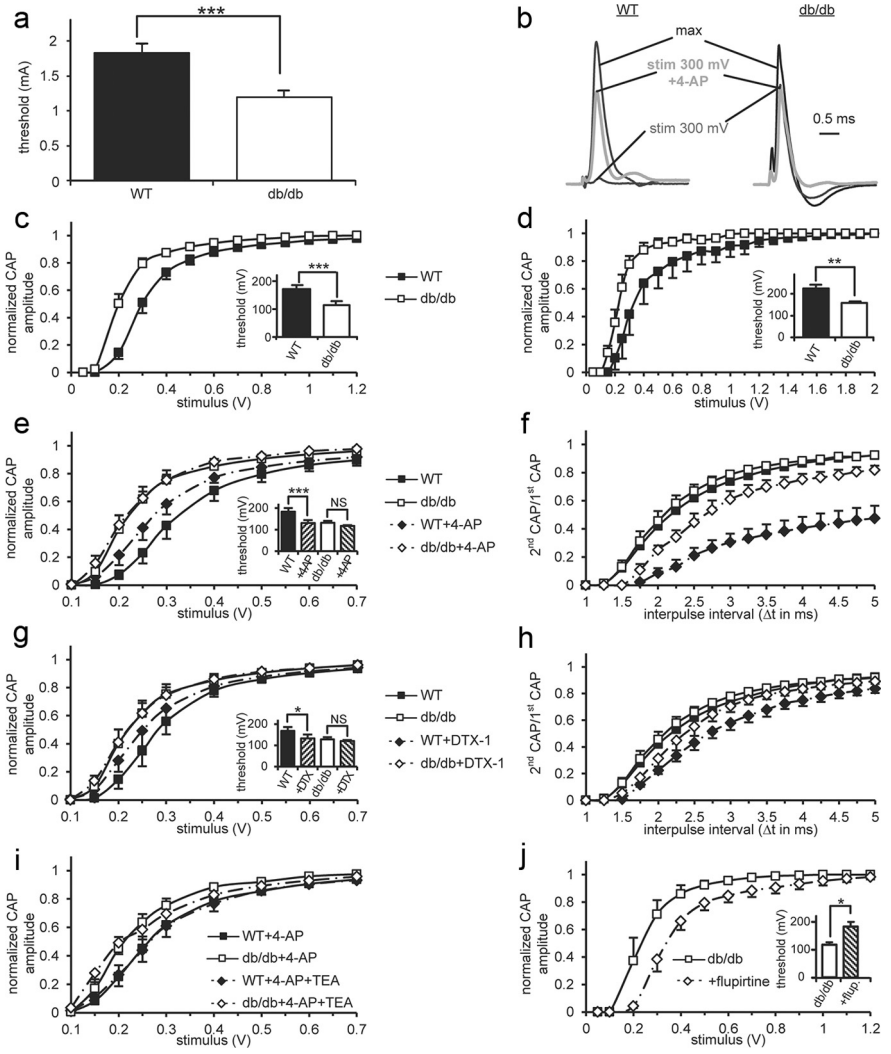

Figure 1. Hyperexcitability of db/db peripheral nerves is mediated by decreased K_v1-channel function. ***a***, *In vivo* measurements of the threshold stimulus to induce a first compound muscle action potential on sciatic nerves. The threshold is significantly decreased in db/db ($n = 20$) compared with WT ($n = 20$) mice. ***b–j***, Data obtained by performing *ex vivo* recordings of compound action potentials (CAPs) on isolated mouse sciatic nerves. All except ***d*** are related to A$\alpha\beta$ CAPs. ***b***, Typical traces of CAPs of WT and db/db nerves at different stimulus strengths (300 mV or the one to get the maximal amplitude) in presence or absence of 4-AP. The amplitudes of the traces are normalized to get the same maximum amplitude in WT and db/db nerves. ***c***, A$\alpha\beta$ CAP amplitude of WT ($n = 11$) and db/db ($n = 12$) nerves normalized by the maximal amplitude as a function of the stimulus strength. We observed a leftward shift of the db/db curve corresponding to peripheral nerve hyperexcitability (PNH). Inset: a significantly reduced threshold in db/db nerves confirms PNH. ***d***, Aδ CAP amplitude/stimulus strength curves. As for larger A$\alpha\beta$ fibers, thinly myelinated Aδ sensory fibers are more excitable in db/db ($n = 5$) compared with WT ($n = 7$) nerves. Inset: the threshold to generate an Aδ CAP is also significantly decreased in db/db nerves. ***e***, 4-AP (500 μM), a blocker of K_v1-channels, induces hyperexcitability in WT ($n = 6$) but not in db/db ($n = 6$) nerves, suggesting decreased function of these juxtaparanodal potassium channels. ***f***, Effect of 4-AP on A$\alpha\beta$ CAP refractory period (RP). The RP is represented as the ratio of the second CAP on the first CAP amplitude (second CAP/first CAP) as a function of the interpulse interval (Δt). 4-AP increases RP significantly more in WT ($n = 6$) than in db/db ($n = 6$) nerves confirming a decrease in K_v1-channel function. ***g***, DTX-1, a toxin specifically blocking K_v1-channels, has a similar effect than 4-AP on db/db and WT nerve excitability ($n = 6$). ***h***, Effect of DTX-1 on RP. As for 4-AP, WT RP ($n = 6$) is more increased by DTX-1 than db/db RP ($n = 6$). ***i***, Effect of coexposure of TEA (10 mM) with 4-AP (500 μM) on nerve excitability. TEA, which blocks nodal K_v7-channels, does not induce any further increase in excitability in WT ($n = 5$) or in db/db ($n = 4$) nerves. Therefore, a change in K_v7-channels is unlikely to be responsible for PNH in db/db nerves. ***j***, Flupirtine (10 μM), an activator of K_v7-channels, significantly decreases db/db nerve excitability ($n = 5$) thus reversing PNH as shown by the curves. Inset: threshold increases back to WT values. Error bars indicate SEM. $^*p < 0.05$; $^{**}p < 0.01$; $^{***}p < 0.001$. Legends for ***c–d***, ***e–f***, and ***g–h*** are shown between them.

et al., 1992; Maljevic et al., 2008), we studied a potential role of these channels in the observed PNH. We evaluated whether TEA (10 mM), which blocks slow potassium currents in axons (Röper and Schwarz, 1989), would in presence of 4-AP induce a further increase in the excitability of WT nerves reaching similar values as observed in db/db nerves. Excitability was not significantly affected by coexposure of 4-AP and TEA either in WT or in db/db nerves (Fig. 1*i*). Therefore, K_v7- and TTX-R Na_v-channels are unlikely key players in the PNH observed in db/db mice.

We tested whether the PNH could be reversed by modulation of potentially preserved ion channels present in db/db nerves. Flupirtine (10 μM), an analgesic activating K_v7-channels, suppressed PNH in db/db nerves as revealed by the increased threshold and stim1/2 ($p < 0.05$, Fig. 1*j*).

Altered channel localization may explain the decreased function of K_v1-channels and the consequent PNH phenotype observed in 23-week-old db/db mice (Devaux, 2010; Shibuya et al., 2011). Therefore, we characterized the K_v1-channel distribution along peripheral axons. Teased fibers of sciatic nerves from 5- and 23-week-old WT mice coimmunostained for $K_v1.2$ and pan-Na_v showed typical accumulation of nodal Na_v-subunits and specific localization of juxtaparanodal $K_v1.2$-subunits (Fig. 2*a*). The same expression pattern was detected in db/db teased fibers at 5 weeks of age before the onset of T2DM and DPN (Fig. 2*a*). Interestingly, we observed a strong reduction of juxtaparanodal $K_v1.2$-subunits in db/db teased fibers at 23 weeks of age, whereas Na_v-clusters were well preserved (Fig. 2*a*). Quantification revealed that 80% of all analyzed nodes present a reduced or absent $K_v1.2$ signal in db/db mice (Fig. 2*a*). Moreover, internodal localization of $K_v1.2$ was also affected in db/db fibers (Fig. 2*b*). However, other K_v1-channel subunits, $K_v1.1$ and $K_v\beta2$, were not affected in db/db mice compared with WT mice and were normally distributed even at juxtaparanodes with reduced or absent $K_v1.2$ (Fig. 2*c*).

Defects in multiple molecular mechanisms can lead to the observed altered distribution of $K_v1.2$-channels and we evaluated some of them. We tested for potential changes in expression of ion channel subunits in DRG and sciatic nerve endoneurium of 23-week-old mice since it was previously shown that the alteration in the distribution of $K_v1.2$ can be due to their decreased expression in the neurons (Shibuya et al., 2011). In DRG, we observed no differences in the mRNA expression levels of $K_v1.2$, $K_v\beta2$ and $Na_v1.6$ (the major subunit of nodal Na_v-channels) while $K_v1.1$ showed a slight upregulation (Fig. 2*d*). Moreover, the protein expression of the mature (glycosylated) and immature isoforms of $K_v1.2$ in DRG and in sciatic nerve endoneurium was similar between db/db and WT mice (Fig. 2*e*) indicating that $K_v1.2$ is normally expressed and transported to the axon. Demyelination is also known to affect juxtaparanodal K_v1-channel

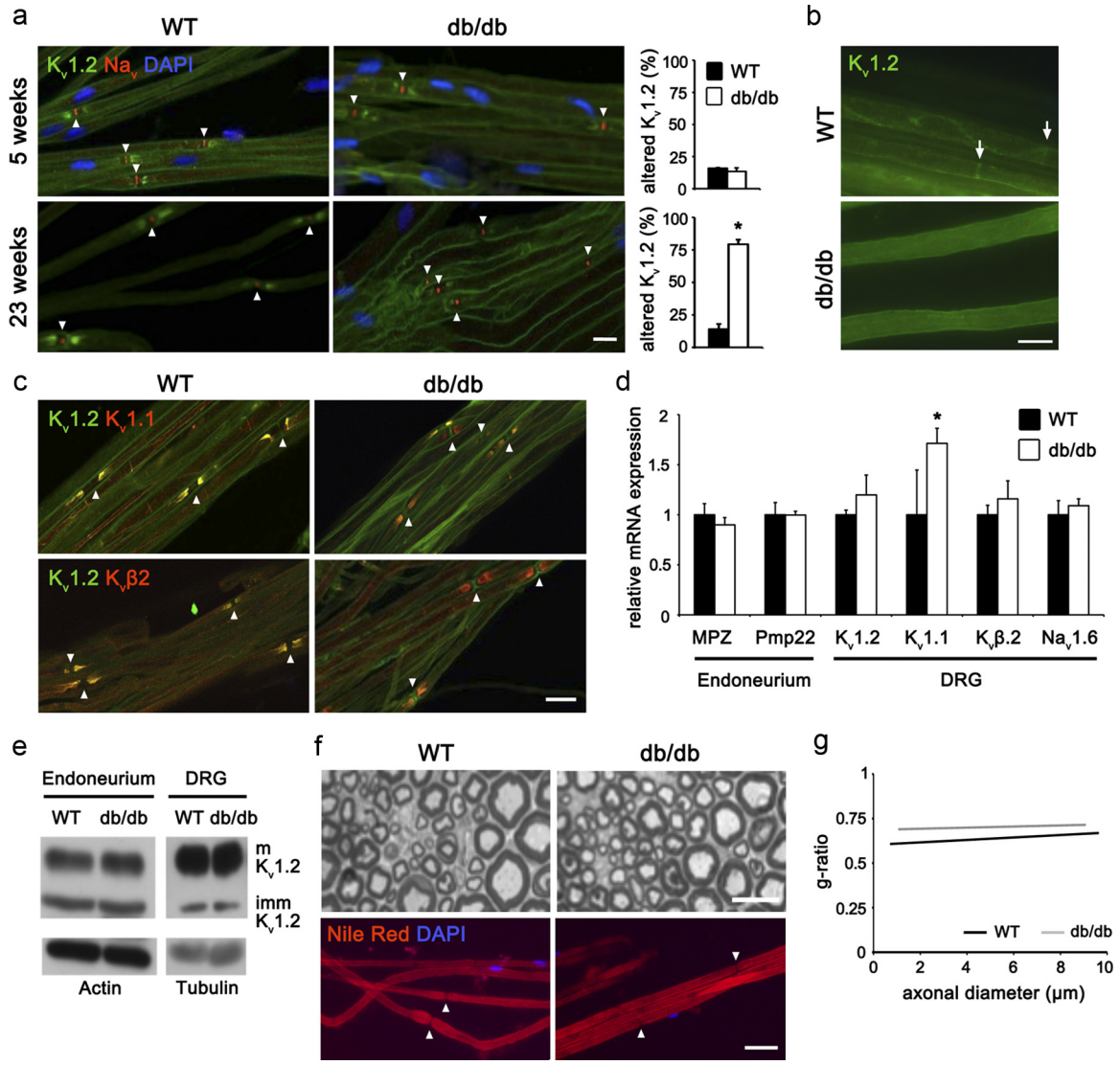

Figure 2. K_v1.2 distribution is altered in db/db mice. ***a***, At 5 weeks of age, before the onset of T2DM and DPN in db/db mice, nodal Na_v-channels and juxtaparanodal K_v1.2-subunits are correctly clustered in teased fibers from both WT ($n = 2$) and db/db mice ($n = 3$). At 23 weeks of age, WT mice ($n = 6$) show the typical expression pattern of K_v1.2 and Na_v but in db/db teased fibers ($n = 6$) the K_v1.2 expression was significantly reduced. However, the nodal Na_v-clusters remained unaffected. Bar graphs on the right illustrate the percentage of juxtaparanodes with reduced or absent K_v1.2 signal of 100 counted nodes. Arrowheads present in ***a***, ***c***, ***f*** mark the localization of nodal regions. ***b***, Internodal K_v1.2 localization is altered in 23-week-old db/db mice compared with age-matched WT mice. Schmidt-Lanterman incisures apposing localization is indicated by arrows. ***c***, At 23 weeks of age, all juxtaparanodal regions show colocalization of K_v1.2 and K_v1.1 or $K_v\beta$2 respectively in WT mice ($n = 3$). While also in db/db mice ($n = 3$) K_v1.1 or $K_v\beta$2 are appropriately positioned in all juxtaparanodal regions, K_v1.2 is lost in some of the regions (red staining). ***d***, qPCR data showing that, except for a mild increase of K_v1.1, all ion channel subunits are normally expressed in db/db compared with WT DRGs ($n = 3$). The peripheral myelin genes MPZ and Pmp22 show no difference in their expression level in db/db and WT sciatic nerve endoneurium. ***e***, K_v1.2 protein expression of both mature and immature isoforms is not reduced in db/db DRGs and sciatic nerve endoneurium compared with WT levels ($n = 3$). ***f***, Toluidine blue-stained semithin cross sections and Nile red-stained teased fibers of WT ($n = 3$) and db/db ($n = 3$) sciatic nerves show that 16 weeks of hyperglycemia has no detectable effect on the axonal and myelin structures. ***g***, The g-ratio corroborates this result ($n = 3$). Scale bars in ***a***, ***c***, ***f***: 20 μm; in ***b***: 8 μm. Error bars indicate SD; $^*p < 0.05$.

clustering (Arroyo et al., 2004). We analyzed the myelin morphology of db/db mice at 23 weeks of age. Semithin cross sections (Fig. 2*f*) and g-ratio [ratio between axonal area and total (axonal + myelin) area] measurements (Fig. 2*g*) as well as qPCR analysis (Fig. 2*d*) for two important peripheral myelin genes (MPZ and Pmp22) failed to reveal any demyelination in db/db mice. Moreover, no segmental demyelination was observed by Nile Red stainings on teased fibers of db/db mice compared with WT mice (Fig. 2*f*). Together these observations indicate that, most probably, the K_v1.2-channel anchoring into the axolemma may be affected under diabetic condition.

To assess the clinical relevance of our data, we evaluated the channel distribution in nerve biopsies from T2DM patients with a predominantly axonal form of DPN (Table 1 and Fig. 3*a*). Co-immunostainings of K_v1.2 and pan-Na_v on longitudinal sections of the peroneal nerve, a major branch of the mixed sciatic nerve, of control subjects revealed the typical accumulation of nodal Na_v-channels and juxtaparanodal K_v1-channels. Similar to the phenotype of db/db mice, we observed a significant reduction of juxtaparanodal K_v1.2-subunits in all analyzed T2DM patients (Fig. 3*a*) while nodal Na_v-clusters were well preserved. Eighty-seven percent of the counted nodes had an impaired or absent K_v1.2 signal in T2DM patients (Fig. 3*a*). Although all T2DM patients presented a loss of myelinated fibers (Table 1), none of them showed obvious signs of segmental demyelination (Fig. 3*b*).

Table 1. Clinical profile of diabetic and control subjects

Patient	Sex	Age (y)	Age of onset of T2DM (y)	Neuropathy	Symptoms	Nerve biopsy
08N01013	M	52	Unaffected by T2DM	—	Neurogenic muscular atrophy, sensory defects until knee, squeezed lateral cutaneous nerve from thigh to spinal cord	Normal
09N01460	F	63	Unaffected by T2DM	—	Chronic neurogenic muscular atrophy, walking/balance problems since 2 years, progressive, sensory defects	Normal
10N00090	M	51	Unaffected by T2DM	Impairment of L5-S1 (bilateral)	Muscular atrophy, disease of vertebral discs, pain, motor and sensory defects	Normal, rare regeneration
08N00894	M	57	54	Axonal	Fast progressive motor defects, sensory defects in lower limbs, amyotrophy	Loss of medium/small size myelinated fibers as well as unmyelinated fibers, WD, infiltration of immune cells
09N01529	F	72	58	Axonal	Progressive motor/sensory defects since 4 years, hypoesthesia, reduced balance/vibration sense	Loss of medium/small size myelinated fibers as well as unmyelinated fibers, signs of WD and microangiopathy
10N00300	M	41	n.d.	Axonal and demyelinating	Paresthesia of lower limbs since 6 months, sensory defects of all four limbs	Moderate loss of large myelinated fibers, WD and edema, inflammatory processes, diabetic microangiopathy

WD, Wallerian degeneration; n.d., not determined; —, not detected.

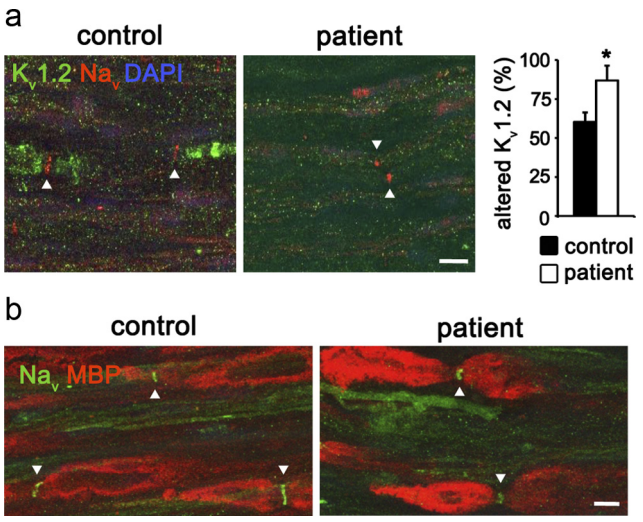

Figure 3. Altered K_v1.2 distribution in peripheral nerves of diabetic patients. ***a***, Longitudinal sections of peroneal nerve biopsies from T2DM ($n = 3$) and control subjects ($n = 3$) were immunostained for Na_v and K_v1.2. In control subjects, Na_v-channels accumulate at the node of Ranvier and K_v1.2-channels at the juxtaparanode. Interestingly, as observed in db/db mice, T2DM patients show a striking loss of juxtaparanodal K_v1.2-channels. The bar graph on the right represents the percentage of juxtaparanodal regions with reduced or abnormal K_v1.2 distribution (100 nodes per controls and subjects were counted). ***b***, Immunostaining for MBP and Na_v on human biopsies did not reveal any presence of segmental demyelination in diabetic subjects. Arrowheads mark the localization of nodal regions. Scale bars: 10 μm. Error bars indicate SD; $^*p < 0.05$.

Discussion

Similar to previously published data (Hummel et al., 1966; Herberg and Coleman, 1977; Robertson and Sima, 1980) we observed a relatively early onset of T2DM in db/db mice. This diabetic phenotype was progressive and accompanied by DPN. Importantly, we have identified, for the first time, the presence of PNH in db/db mice thus validating it as a model to characterize this part of the DPN phenotype. Similar to the situation in diabetic patients where PNH is thought to be responsible of the positive symptoms (Quasthoff, 1998; Misawa et al., 2005, 2009), it could explain allodynia in db/db mice (Cheng et al., 2009).

Using *ex vivo* CAP recordings, we have clearly demonstrated that a reduced activity of K_v1-channels was involved in the PNH phenotype of db/db mice. A role of other channels (e.g., K_v7.2 or Na_V-channels) is unlikely critical but cannot be completely ruled out. K_v1-channels are clustered at the juxtaparanodal regions and along the internodes of myelinated peripheral axons (Salzer, 2003). It was previously observed that paranodal/juxtaparanodal potassium binding sites are reduced in nerves from diabetic patients (Seneviratne and Weerasuriya, 1974). We have specifically shown that the K_v1.2 distribution is altered in both db/db mice and in T2DM nerve biopsies thus providing, to our knowledge, the first direct demonstration of such an alteration in axonal ion channels in diabetic patients. Importantly, previous clinical studies already demonstrated that alterations in K_v1-channel function may lead to PNH or myokymia in different pathological situations (Arimura et al., 2002; Tomlinson et al., 2010; Shibuya et al., 2011).

We excluded a reduction of K_v1.2 expression in the soma of neurons as the cause of the decreased K_v1.2 signal in axons. Furthermore, we did not observe any accumulation of K_v1.2 subunits in DRG of db/db mice and its expression (as detected by Western blot) was normal in sciatic nerve endoneurium suggesting that axonal targeting of K_v1.2 is not responsible for the phenotype. We also clearly excluded a demyelinating phenotype in db/db and human nerves as being the cause of the altered K_v1.2 distribution. Interestingly, it was previously observed that the absence of Caspr2 or TAG-1, two adhesion molecules responsible for the juxtaparanodal targeting of K_v1.2, lead to redistribution of K_v1.2-channels to the internodal regions (Poliak et al., 2003). However, in db/db mice even the internodal K_v1.2 localization is affected suggesting that the diabetic condition leads to a diffuse K_v1.2 distribution along the axolemma. As opposed to most ion channel subunits which possess intrinsic targeting motifs, both the membrane targeting and TAG1-mediated clustering of K_v1.2 is mainly dependent on its phosphorylation status (Gu and Gu, 2011) which might be affected under diabetic condition. Further experiments are therefore needed to clarify the mechanisms underlying the observed K_v1.2 mislocalization.

Our data indicate at least two different approaches how to improve DPN condition (particularly PNH) for which there are no effective therapies. First, one may try to enhance the targeting of K_v1.2 to its juxtaparanodal and internodal locations thus improving the hypersensitivity phenotype. Alternatively, our expression and pharmacology data generated in db/db mice

showed that there are multiple ion channel-types (including Na_v1.6, K_v1.1, K_v7.2 and K_v7.3) that are well preserved in the diabetic peripheral nerve. Both the inhibition of Na_v-channels and the activation of preserved K_v-channels might alleviate the PNH phenotype. We validated the clinical potential of the second approach by suppressing PNH in db/db nerves with the K_v7-activator flupirtine. Interestingly, flupirtine, which is an analgesic, has been shown previously to suppress PNH resulting from exposure of rat and human peripheral nerves to oxaliplatin (Sittl et al., 2010).

In conclusion, we demonstrated that K_v1-channels, particularly K_v1.2, play a critical role in the PNH phenotype of db/db mice and corroborated these data with the characterization of biopsies from T2DM patients. We anticipate that these results may have direct clinical implications for the development of new treatments against T2DM-related PNH.

References

Arimura K, Sonoda Y, Watanabe O, Nagado T, Kurono A, Tomimitsu H, Otsuka R, Kameyama M, Osame M (2002) Isaacs' syndrome as a potassium channelopathy of the nerve. Muscle Nerve [Suppl 11]:S55–S58.

Arnaud E, Zenker J, de Preux Charles AS, Stendel C, Roos A, Médard JJ, Tricaud N, Kleine H, Luscher B, Weis J, Suter U, Senderek J, Chrast R (2009) SH3TC2/KIAA1985 protein is required for proper myelination and the integrity of the node of Ranvier in the peripheral nervous system. Proc Natl Acad Sci U S A 106:17528–17533.

Arroyo EJ, Sirkowski EE, Chitale R, Scherer SS (2004) Acute demyelination disrupts the molecular organization of peripheral nervous system nodes. J Comp Neurol 479:424–434.

Cartoni R, Arnaud E, Médard JJ, Poirot O, Courvoisier DS, Chrast R, Martinou JC (2010) Expression of mitofusin 2(R94Q) in a transgenic mouse leads to Charcot-Marie-Tooth neuropathy type 2A. Brain 133:1460–1469.

Cheng HT, Dauch JR, Hayes JM, Hong Y, Feldman EL (2009) Nerve growth factor mediates mechanical allodynia in a mouse model of type 2 diabetes. J Neuropathol Exp Neurol 68:1229–1243.

de Preux Charles AS, Verdier V, Zenker J, Peter B, Médard JJ, Kuntzer T, Beckmann JS, Bergmann S, Chrast R (2010) Global transcriptional programs in peripheral nerve endoneurium and DRG are resistant to the onset of type 1 diabetic neuropathy in Ins2 mice. PLoS One 5:e10832.

Devaux J, Gow A (2008) Tight junctions potentiate the insulative properties of small CNS myelinated axons. J Cell Biol 183:909–921.

Devaux JJ (2010) The C-terminal domain of ssIV-spectrin is crucial for KCNQ2 aggregation and excitability at nodes of Ranvier. J Physiol 588:4719–4730.

Gu C, Gu Y (2011) Clustering and activity tuning of Kv1 channels in myelinated hippocampal axons. J Biol Chem 286:25835–25847.

Herberg L, Coleman DL (1977) Laboratory animals exhibiting obesity and diabetes syndromes. Metabolism 26:59–99.

Hummel KP, Dickie MM, Coleman DL (1966) Diabetes, a new mutation in the mouse. Science 153:1127–1128.

Maljevic S, Wuttke TV, Lerche H (2008) Nervous system KV7 disorders: breakdown of a subthreshold brake. J Physiol 586:1791–1801.

Matsutomi T, Nakamoto C, Zheng T, Kakimura J, Ogata N (2006) Multiple types of Na(+) currents mediate action potential electrogenesis in small neurons of mouse dorsal root ganglia. Pflugers Arch 453:83–96.

Misawa S, Kuwabara S, Kanai K, Tamura N, Hiraga A, Nakata M, Ogawara K, Hattori T (2005) Axonal potassium conductance and glycemic control in human diabetic nerves. Clin Neurophysiol 116:1181–1187.

Misawa S, Sakurai K, Shibuya K, Isose S, Kanai K, Ogino J, Ishikawa K, Kuwabara S (2009) Neuropathic pain is associated with increased nodal persistent Na(+) currents in human diabetic neuropathy. J Peripher Nerv Syst 14:279–284.

Nolan CJ, Damm P, Prentki M (2011) Type 2 diabetes across generations: from pathophysiology to prevention and management. Lancet 378:169–181.

Poliak S, Salomon D, Elhanany H, Sabanay H, Kiernan B, Pevny L, Stewart CL, Xu X, Chiu SY, Shrager P, Furley AJ, Peles E (2003) Juxtaparanodal clustering of Shaker-like K+ channels in myelinated axons depends on Caspr2 and TAG-1. J Cell Biol 162:1149–1160.

Quasthoff S (1998) The role of axonal ion conductances in diabetic neuropathy: a review. Muscle Nerve 21:1246–1255.

Robertson DM, Sima AA (1980) Diabetic neuropathy in the mutant mouse [C57BL/ks(db/db)]: a morphometric study. Diabetes 29:60–67.

Röper J, Schwarz JR (1989) Heterogeneous distribution of fast and slow potassium channels in myelinated rat nerve fibres. J Physiol 416:93–110.

Salzer JL (2003) Polarized domains of myelinated axons. Neuron 40:297–318.

Schwarz JR, Glassmeier G, Cooper EC, Kao TC, Nodera H, Tabuena D, Kaji R, Bostock H (2006) KCNQ channels mediate IKs, a slow K+ current regulating excitability in the rat node of Ranvier. J Physiol 573:17–34.

Seneviratne KN, Weerasuriya A (1974) Nodal gap substance in diabetic nerve. J Neurol Neurosurg Psychiatry 37:502–513.

Shibuya K, Misawa S, Arai K, Nakata M, Kanai K, Yoshiyama Y, Ito K, Isose S, Noto Y, Nasu S, Sekiguchi Y, Fujimaki Y, Ohmori S, Kitamura H, Sato Y, Kuwabara S (2011) Markedly reduced axonal potassium channel expression in human sporadic amyotrophic lateral sclerosis: An immunohistochemical study. Exp Neurol 232:149–153.

Sittl R, Carr RW, Fleckenstein J, Grafe P (2010) Enhancement of axonal potassium conductance reduces nerve hyperexcitability in an in vitro model of oxaliplatin-induced acute neuropathy. Neurotoxicology 31:694–700.

Stys PK, Ransom BR, Waxman SG (1991) Compound action potential of nerve recorded by suction electrode: a theoretical and experimental analysis. Brain Res 546:18–32.

Taylor JL, Burke D, Heywood J (1992) Physiological evidence for a slow K+ conductance in human cutaneous afferents. J Physiol 453:575–589.

Tomlinson SE, Tan SV, Kullmann DM, Griggs RC, Burke D, Hanna MG, Bostock H (2010) Nerve excitability studies characterize Kv1.1 fast potassium channel dysfunction in patients with episodic ataxia type 1. Brain 133:3530–3540.

Vabnick I, Trimmer JS, Schwarz TL, Levinson SR, Risal D, Shrager P (1999) Dynamic potassium channel distributions during axonal development prevent aberrant firing patterns. J Neurosci 19:747–758.